The Laplace multi-axial response model for fatigue analysis

Karlsson, Johan; Podgorski, Krzysztof; Rychlik, Igor

2015

Working Papers in Statistics
No 2015:8
Department of Statistics
School of Economics and Management
Lund University

The Laplace multi-axial response model for fatigue analysis

JOHAN KARLSSON, FRAUNHOFER-CHALMERS CENTRE FOR INDUSTRIAL MATHEMATICS
KRZYSZTOF PODGÓRSKI, LUND UNIVERSITY
IGOR RYCHLIK, CHALMERS UNIVERSITY OF TECHNOLOGY

The Laplace multi-axial response model for fatigue analysis

Johan Karlsson[1], Krzysztof Podgórski[2], and Igor Rychlik[3]

[1] Fraunhofer-Chalmers Centre for Industrial Mathematics, SE-412 88 Gothenbourg, Sweden, johan.karlsson@fcc.chalmers.se
[2] Statistics, Lund University, 220 07 Lund, Sweden, krzysztof.podgorski@stat.lu.se
[3] Mathematical Sciences, Chalmers University of Technology, SE-412 96 Göteborg, Sweden, rychlik@chalmers.se

Abstract. This paper introduces means for fatigue damage rates estimation using Laplace distributed multiaxial loads. The model is suitable for description of stresses containing transients of random amplitudes and locations. Explicit formulas for computing the expected value of rainflow damage index as a function of excess kurtosis are given for correlated loads. A Laplace model is used to describe variability of forces and bending moments measured at some location on a cultivator frame. An example of actual cultivator data is used to illustrate the model and demonstrate the accuracy of damage index prediction.

Keywords: Laplace moving averages, multi-axial loads, rainflow method, random loading, spectral density function

List of symbols

a	– spectrum scale parameter (dimensionless)
β	– damage exponent (dimensionless)
$\mathbf{c} = (c_1, \ldots, c_M)$	– constants combining loads into stress: $10^6\times$ [m^{-3}] (bending moments), $10^6\times$ [m^{-2}] (forces)
$D(\mathbf{c}) = D_{\mathbf{X}}(\mathbf{c})$	– rainflow multiaxial damage index [m^{β}/s]
$D^{obs}(\mathbf{c})$	– observed multiaxial damage index [m^{β}/s]
$\mathscr{D}(\mathbf{c}) = \mathscr{D}_{\mathbf{X}}(\mathbf{c})$	– expected damage index [m^{β}/s]
F_x, F_y, F_z	– forces in the principal directions [N]
$\mathscr{F}$, $\mathscr{F}^{-1}$,	– Fourier transform and its inverse
$g(t)$	– kernel for scale standardized moving averages
$\Gamma(\cdot)$	– gamma function
$h_k^{rf}(\mathbf{c}),\ k = 1, \ldots, K$	– the rainflow cycle ranges [m]
κ, κ_e	– kurtosis and excess kurtosis of a load (dimensionless)
M_x, M_y, M_z	– bending moments in the principal directions [Nm]
ν	– shape parameter in gamma distribution
ω	– angular frequency [rad]
$\mathbf{R} = [R_i]$	– gamma white noise
ρ	– correlation in bivariate noise $[\mathbf{W}_1, \mathbf{W}_2]$
σ^2	– variance of the load [$\mathrm{N}^2\mathrm{m}^2$] or [N^2]
Σ	– covariance matrix of the bivariate load [$\mathrm{N}^2\mathrm{m}^2$] or [N^2]
$S_a(\omega)$	– spectrum of bending moment load [$\mathrm{N}^2\mathrm{m}^2$/rad]
$S(\omega)$	– normalized spectrum of a load [rad^{-1}]
t, T	– running time, total time, respectively, [s]
$\mathbf{X}(t) = (X_1(t), \ldots, X_M(t))$	– vector of loads: bending moments [Nm], forces [N]
$\mathbf{X}^{obs}(t)$	– observed loads: bending moments [Nm], forces [N]
$X(t)$	– scale normalized dimensionless load
$Y_{\mathbf{c}}(t)$	– stress [MPa]
$\mathbf{W} = [W_i]$	– white noise (independent equally distributed random variables)
$[\mathbf{W}_1, \mathbf{W}_2]$	– white noise in the bivariate case
$\mathbf{Z} = [Z_i]$	– Gaussian white noise

1 Introduction

Stochastic modeling of loads is usually done with stationary Gaussian processes. Well-developed numerical tools for computing the probabilities of interests are available, see e.g. [1]. However, many of the environmental loads that act on for example ground vehicles are far from being Gaussian. Nevertheless, Gaussian models are often used, and this sometimes leads to serious underestimation of risks for fatigue.

Estimations of component durability often requires a customer or market specific load description. One is interested in having models that are capable of describing the correct variability of loads with a relatively small number of parameters. These models can then be used to describe the long term loading by means of a distribution of the parameter values, specific for a given market or encountered by specific customers.

The severity of environmental loads can be measured by means of damage indexes. In the case when Gaussian models are used for stresses, there are many methods for estimating the expected damage indexes from the power spectrum density, psd, see eg. [2] for a review of different approaches. Much less is known for loads containing transients. In this paper, explicit formulas for computing expected value of rainflow damage index as a function of excess kurtosis will be given, for a special case of equally distributed although correlated Laplace loads.

A Gaussian model can be seen as the result of smoothing Gaussian white noise, i.e a sequence of independent standard Gaussian variables, by a suitable kernel. When a cultivator is operating in light sandy soils where stones are frequent, the vibrations have a larger spread of variation that can not be modeled by solely Gaussian processes. The Laplace white noise is used to model the larger spread by letting Gaussian white noise have variable variance. This is achieved by multiplying the Gaussian variables by the square root of gamma distributed factors. The factors have mean value one, and hence, loads derived by smoothing Gaussian or Laplace noise with the same kernel will have

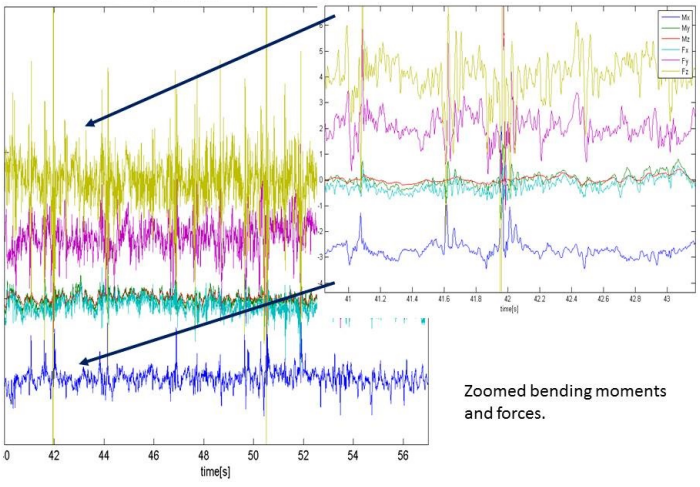

Fig. 1. Measured forces and bending moments at one location of cultivator frame

identical power spectrum densities (psd). However, in contrast to the Gaussian process, the Laplace process will have visible transients at times when factors take large values.

In this paper, we present models for loads, which are forces and bending moments, measured at some point of a stiff mechanical structure.For example, the method is used to asses the durability of welds in a stiff frame of a cultivator. Hence accurate description of stress variability at welds are needed. For a stiff frame, stresses are linear combinations of environmental loads. This property makes modeling using Gaussian processes very convenient, since linear combinations of Gaussian loads are Gaussian processes as well and any probability of interest can in principle be computed when the psd of the loads are available.

In Figure 1, six loads, measured on one tine, are presented. In the figure one can see that transients appearing in different forces and bending moments are often close in time. Since stress is a linear combination of the loads this may result in very large stresses which may greatly amplify the damage accumulation rate. The proposed multiaxial Laplace model for load will have the property of high frequency of simultaneous occurrences of large transients. Table 1 shows statistics for the dominating signals.

Load	St. deviation	Kurtosis	Parameter a in (3)	Damage index $D^{obs}(1)$
F_y	0.72	11.4	0.012	369
F_z	0.77	9.4	0.009	518
M_x	0.39	20.1	0.015	56

Table 1. Statistics of loads presented in Figure 1.

2 Fatigue damage

In this paper, multivariate random processes $\mathbf{X}(t) = (X_1(t), \ldots, X_M(t))$ are used to represent multi-axial loads, being forces and bending moments acting on a structure at different locations. For a stiff structure, stresses, used to predict fatigue damage, are linear combinations of forces and moments. For this reason, it is important to model the multi-axial load so that a stress, i.e. a linear combination of loads

$$Y_{\mathbf{c}}(t) = \sum_{r=1}^{M} c_r X_r(t), \qquad t \in [0,T], \tag{1}$$

yields accurate fatigue accumulation. In the examples in this paper we focus on the situation where the sum above is over forces and moments measured at one position. If there are forces and moments in several positions, the sum should be over all of them. Since the vector $\mathbf{c} = (c_1, \ldots, c_M)$ may vary between locations in a structure experiencing the same loads $\mathbf{X}(t)$ one requires good accuracy for any choice of constants $\mathbf{c}$. These are typically evaluated using finite elements method and depend on geometry and material properties and transfer external loads to stresses at a point in the structure of interest.

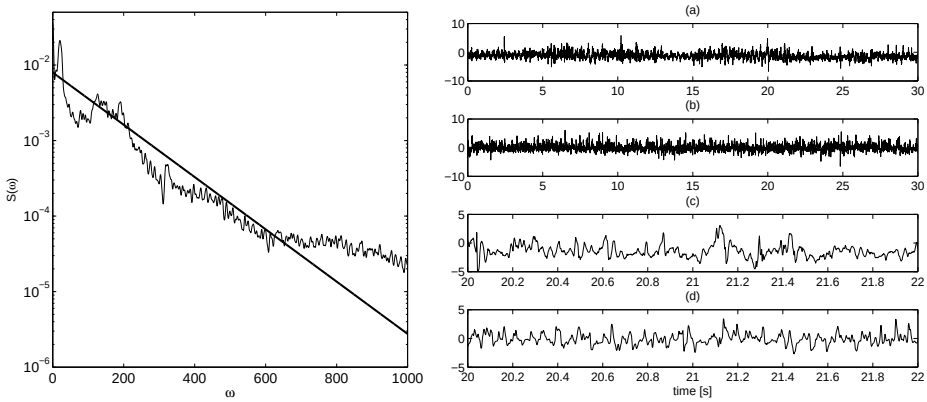

Fig. 2. *Left:* Logarithms of empirical psd of $F_z(t)$ (thin irregular line) and fitted exponential psd (thick straight line). *Right:* Plot (a) - one minute of one measured force on a cultivator frame. Plot (b) - one minute of simulated LMA model of the force. Plot (c) - zoomed plot (a). Plot (d) zoomed plot (b).

The fatigue damage accumulated in the material is expressed using a fatigue (damage) index defined by means of the rainflow method which is computed in the following two steps. First, rainflow ranges $h_k^{rf}(\mathbf{c})$, $k = 1,\ldots,K$, in $Y_{\mathbf{c}}(t)$ are found. Here K is the number of rainflow cycles which equals the number of local maxima. Then the rainflow damage is computed according to Palmgren-Miner rule [3], [4], viz.

$$D(\mathbf{c}) = \frac{1}{T}\sum_{k=1}^{K}(h_k^{rf}(\mathbf{c}))^{\beta}, \tag{2}$$

see also [5] for details of this approach. Various choices of the damage exponent β can be considered. The value is an empirical constant estimated by means of regression from experiments involving constant amplitude loads. In this paper $\beta = 3$, which is the standard value for the crack growth process in a welded frame. The index $D(\mathbf{c})$ is often called multi-axial damage index and was introduced in [6].

The proposed model for the multi-axial loads $\mathbf{X}(t)$ is validated by using measured loads and comparing the ensuing damage index with the expected value of the damage index following from the model fitted to the data. In this, first the model parameters are estimated using measured loads $\mathbf{X}^{obs}(t)$. Then the expected theoretical damage index $\mathscr{D}(\mathbf{c}) = \mathsf{E}[D(\mathbf{c})]$ is estimated by means of Monte Carlo (MC) method and compared with $D^{obs}(\mathbf{c})$ for a suitably chosen vector of factors $\mathbf{c}$, where $D^{obs}(\mathbf{c})$ is computed by means of (2) with rainflow ranges obtained in the observed records. In our notation, we do not explicitly indicate that the expected damage index $\mathscr{D}(\mathbf{c})$ depends also on the properties and defining parameters of the process $\mathbf{X}$. In what follows, whenever this dependence needs to be exhibited, we write $D_{\mathbf{X}}(\mathbf{c})$ and $\mathscr{D}_{\mathbf{X}}(\mathbf{c})$ for the damage and the expected damage, respectively.

3 Uniaxial load

Power spectral density (psd) is an important characteristics of stationary stress (load). For Gaussian stress the fatigue damage index is a function of psd alone. Even for Laplace processes, psd remains an important characteristic. However, it in general does

not determine the damage index completely. In this paper, a very simple, yet often used, reparametrization of the model for psd is used

$$S_a(\omega) = \sigma^2 a S(a\omega) \qquad a > 0, \tag{3}$$

where $\int S(\omega)\,d\omega = 1$, σ^2 is the variance of the load, while a is a spectrum scale parameter. A load with psd given in (3) can be written as

$$X_a(t) = \sigma X(t/a), \tag{4}$$

where $X(t) = X_1(t)/\sigma$, having psd $S(\omega)$, is a scale normalized load. The psd (3) and process (4), where $X(t)$ is Laplace moving average, have found applications, for example, in road roughness classifications, where a is the velocity a vehicle travels while $S(\omega)$ depends on the linear filter that has been used to model responses and the spectral properties of a road profile, see [7].

The proposed model is applicable to an arbirtrary form of spectrum $S(\omega)$. For modeling cultivator loads, the following psd proves to be useful

$$S(\omega) = 0.5\exp(-|\omega|), \tag{5}$$

see Figure 2, left plot, where the observed psd of the force $F_z(t)$ is compared with the exponential psd. In the right plot a simulation using the Laplace model for the force is presented. Although not all visual properties of $F_z(t)$ can be found in the simulated signal, the damage index of the measured load is very close to the expected damage index of the Laplace model, see Table 2 for values of the two indexes.

DAMAGE INDEX			
Data	F_y	F_z	M_x
observed	369	518	56
Laplace model	335	497	56
Gaussian model	151	245	19

Table 2. Observed damage index for loads F_y, F_z, M_x compared with the expected damage indexes for Laplacian and Gaussian models. The loads have psd (5) defined by parameters (a_{Fy}, a_{Fz}, a_{Mx}) equal to $(0.012, 0.09, 0.015)$ and kurtosis and variances given in Table 1

There are many ways to generate a random process X having psd $S(\omega)$. The most direct way is by smoothing white noise $W(t)$, with kernel $g(t) = \mathscr{F}^{-1}(\sqrt{2\pi S(\omega)})$, where $\mathscr{F}$ is the Fourier transform. For the particular case of exponential spectrum this leads to

$$g(t) = \frac{2/\sqrt{\pi}}{1+4t^2}. \tag{6}$$

Approximately, using discretization, a simulated load $\mathbf{X} = [X(t_i)]$, where $t_{i+1} - t_i = dt$, is the convolution of a vector $\mathbf{g} = [g(t_i)]$ with sampled white noise $\mathbf{W} = [W_i]$ multiplied by $\sqrt{dt}$, viz.

$$\mathbf{X} = \sqrt{dt} \cdot \mathbf{g} * \mathbf{W}, \tag{7}$$

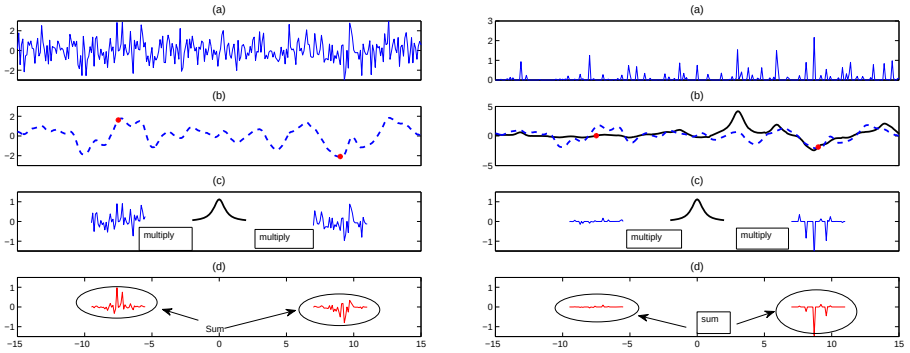

Fig. 3. Illustration of the evaluation of the load having psd (5). Dashed line in plots (b) are Gaussian load while solid line in the plot (b) is the Laplace load. *Left:* Gaussian model; *Right:* Laplace model with kurtosis $\kappa = 8$.

where "$*$" is the convolution of two vectors. Here W_i are independent equally distributed random variables having mean zero and variance one.

3.1 Gaussian model

A Gaussian load is obtained by using Gaussian white noise, i.e. $W_i = Z_i$ where Z_i are standard Gaussian variables. A thus defined Gaussian load X has approximately the psd given in (5), with mean zero, variance one and kurtosis $\kappa = E[X_i^4] = 3$.

In Figure 3, left plot, an illustration of the construction of the Gaussian load using the model given in Eq. (7) is presented. In plot (a) a sampled white noise $\mathbf{W}$ is plotted while in plot (b) the Gaussian load $\mathbf{X}$ is given. The plots (c) and (d) illustrate how the values of loads, marked as dots in plot (b), are evaluated. These are derived by first extracting the noise around the locations and then multiplying it by the kernel $\mathbf{g}$, which gives the two signals presented in plots (d). Secondly the Gaussian load is obtained by calculating the total sum of the signals from plot (d).

3.2 Laplace model

A Laplacian load is obtained using (7) with W_i being Laplace distributed variables, see [8] for the properties of the Laplace distribution. The Laplace noise can be constructed using Gaussian noise Z_i and multiplying Z_i by the square root of a gamma distributed random factor R_i, viz. $W_i = \sqrt{R_i}\,Z_i$. We consider the gamma probability density function parametrized by k so that

$$f(x) = \frac{k^k x^{(k-1)}}{\Gamma(k)} \exp(-kx), \qquad k > 0, \quad x \geq 0 \tag{8}$$

where $\Gamma(k)$ is the gamma function $\Gamma(k) = \int_0^\infty t^{k-1} e^{-t} dt$. The parameters in the distribution of R_i are defined by means of two conditions; that the mean value of R_i has to be

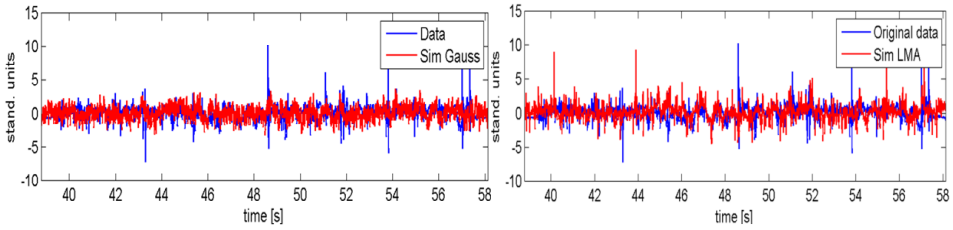

Fig. 4. *Left:* Standardized force F_y compared with Gaussian model having psd (5). *Right:* The force F_y compared with Laplace model having psd (5) and kurtosis $\kappa = 11$.

one and that kurtosis κ of the Laplace model has to agree with kurtosis of the observed load. These two conditions leads to the following parameter values

$$k = \frac{dt}{\nu}, \quad \text{where} \quad \nu = 0.42(\kappa - 3)\, a, \tag{9}$$

see [9] for more detailed presentation. Note that as κ tends to 3 the Laplace model approaches the Gaussian model.

In Figure 3, right plot, illustration of the construction of the Laplace load, defined in (7) is given. In plot (a) gamma distributed factors R_i are shown while in plot (b) the Gaussian load $\mathbf{X}$ (dashed line) is compared with the Laplace load computed using (7) and noise $W_i = \sqrt{R_i} Z_i$. The values of Z_i are given in left plot figure (a). The plots (c) and (d) illustrate how the values of the Laplace load, marked as dots in plot (b), are evaluated. These are derived by extracting the factors R_i around the locations, taking square root of the factors, multiplying those pointwise with the Gaussian noise presented in left plot figure (c) and finally the resulting Laplace noises are multiplied by the kernel $\mathbf{g}$. These operations gave two signals presented in figure (d). Finally the Laplace loads were obtained by summing the signals.

3.3 Damage index

The expected damage index (10) for the Laplace load having psd (5) has been derived in [9] by means of (4) and regression fit to MC simulations of damages for different values of kurtosis κ. The multiplicative structure of (10) makes it very convenient for studying uncertainties in fatigue life predictions, viz.

$$\mathscr{D}_X(c) \approx a^{-1} (c \cdot \sigma)^3 \cdot (4.84 + 0.025\kappa_e + 3.486\kappa_e^{1/2} - 2.158\kappa_e^{1/3}), \tag{10}$$

where $\kappa_e = \kappa - 3$ is the excess kurtosis. For Gaussian load $\kappa_e = 0$.

For illustration of applicability of the formula (10) we consider the simple case where we only have the force F_y presented in Figure 1 ($c = 1$). The force is normalized to have zero mean and variance one and is presented in Figure 4 in blue. The observed damage index is $D^{obs}(1) = 989$. The fitted model gives the estimated parameter $a = 0.012$ and kurtosis $\kappa = 11.4$. Evaluating (10) the expected damage index is $\mathscr{D}(1) = 897$. The value is very close to the observed damage index. Using the Gaussian model having $\kappa = 3$ and the same spectral parameter $a = 0.012$ the approximation (10) gives

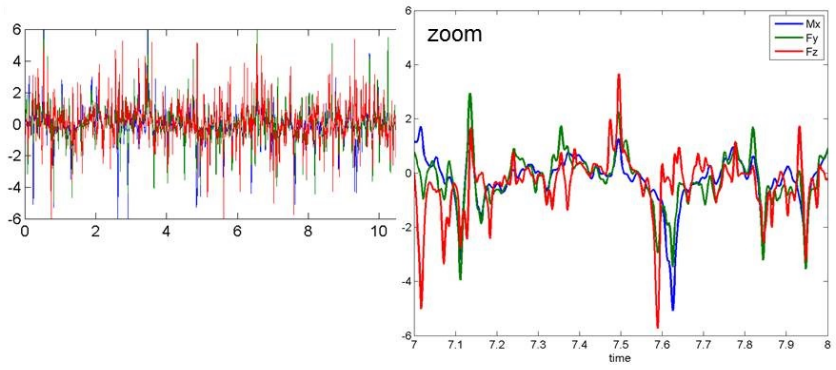

Fig. 5. *Left:* Simulation of the Laplace model for standardized loads (F_y, F_z, M_x), having mean zero and variance one. The loads have individual power spectrums (5) defined by parameters (a_{Fy}, a_{Fz}, a_{Mx}) equal to $(0.012, 0.009, 0.015)$. The kurtosis of the loads are $(\kappa_{Fy}, \kappa_{Fz}, \kappa_{Mx})$ equal to $(11.4, 9.4, 20.1)$. The loads are correlated. Correlation between M_x and F_y is 0.9; M_x and F_z is 0.3; correlation F_y and F_z is 0.5.

$\mathscr{D}(1) = 403$. In this case it is clear that the Gaussian model severely underestimates the damage index.

In Figure 4 the Gaussian and Laplacian simulations are compared with the observed force F_y. The red line in the left plot is the simulation using the Gaussian model and the red line in the right plot is the simulation using the Laplacian model of the force. The blue line is the observed load in both plots. One can see that the transients observed in the load are missing in the simulation using the Gaussian model while these are present when using the Laplace model.

For completeness we list the expected damage indexes, given by (10), for loads presented in Table 1. The results are presented in Table 2. One can see that the Laplace model have expected damage indexes close to the observed ones while the Gaussian model severely underestimates the damages.

4 Multiaxial load

Independent Laplace loads can be simulated by means of the methods given in Section 3.2, using independent Gaussian noises and gamma factors. However, as mentioned before, an important property of the measured loads is that the transients tend to occur simultaneously in the loads. This is an important property that the multiaxial model of loads should possess.(Obviously the independent Laplace loads are lacking the property.) In [10] the general multiaxial Laplace model was given. An example of multiaxially simulated forces F_y, F_z and moment M_x can bee seen in Figure 5.

The general construction of multiaxial Laplace loads is more complex than the uniaxial loads and hence here we shall limits ourself to the simplest special case of bi-axial Laplace loads $(X_1(t), X_2(t))$. A further restriction is that both loads have the same psd (5) and have equal kurtosis. Under the assumed limitations the Laplace loads will be

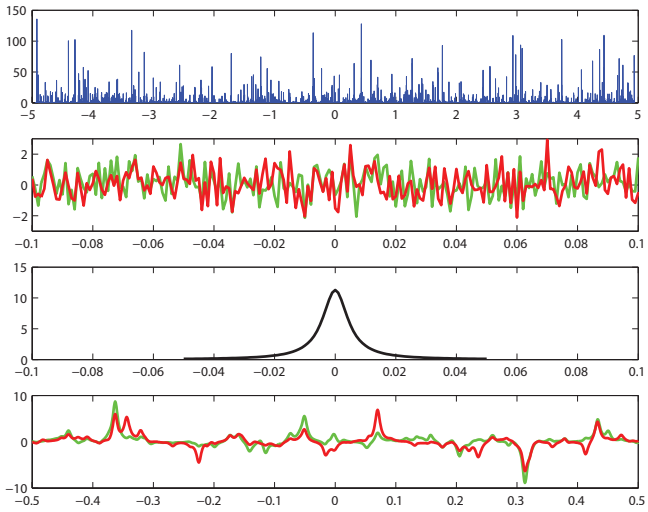

Fig. 6. Illustration of simulation of standardized loads (F_y, F_z) having psd (5) with $a = 0.01$, kurtosis $\kappa = 10$ variance one and mean zero. The loads have correlation $\rho = 0.5$. Figure (a) shows sequence of factors R_i. Figure (b) presents two Gaussian white noise sequences having correlation 0.5. Figure (c) shows the kernel g. Figure (d) shows the simulated correlated Laplace loads.

generated using kernel g given in (6) convoluted with two correlated series of Laplace noises, see (7). In order to assure that the transients will often occur simultaneously in the loads, a common sequence of factors R_i is used in construction of the noises. Two correlated Gaussian noises are generated. Then the Laplace noises are derived by scaling the correlated Gaussian white noises by the square root of the common factors R_i. An example of the construction of correlated Laplace noises is given in Figure 6. In the figure plot (a) shows the common factors. The correlated series of Gaussian white noises are shown in plot (b). The kernel g can be found in plot (c) and finally the two Laplace loads are shown in plot (d).

For completion an algorithm to construct correlated Laplace white noise sequences is given. Let $\mathbf{Z_1}$ and $\mathbf{Z_2}$ be two independent Gaussian white noise sequences. The correlated Laplace white noise sequences $\mathbf{W_1}$ and $\mathbf{W_2}$ are defined as follows

$$W_{1i} = \sqrt{R_i}\,(a_1 Z_{1i} + a_2 Z_{2i})\,, \qquad W_{2i} = \sqrt{R_i}\,(a_2 Z_{1i} + a_1 Z_{2i})\,, \tag{11}$$

where

$$a_1 = \left(\sqrt{1+\rho} + \sqrt{1-\rho}\right)/2, \qquad a_2 = \left(\sqrt{1+\rho} - \sqrt{1-\rho}\right)/2 \tag{12}$$

and ρ is correlation between the loads, see [10] for more details.

In [10] it is also proved that for Laplace loads with common parameters a and kurtosis κ the expected damage index for damage exponent $k = 3$ can be approximated as follows

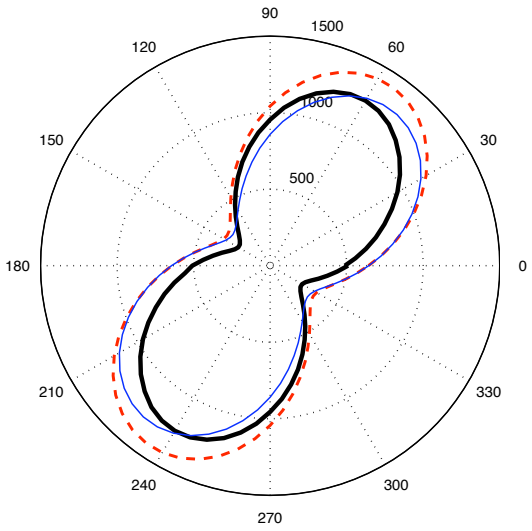

Fig. 7. *Thick solid line:* observed $D(\mathbf{c})$ (in 18 measured loads sequences), where $\mathbf{c} = [\cos(\theta)\ \sin(\theta)]$. *Dashed line:* average $D(\mathbf{c})$ (simulated) using individual parameters for the 18 multiaxial measured loads. *Thin solid line:* the approximation $\mathscr{D}(\mathbf{c})$, average kurtosis, average psd were and average correlation between the measured loads used. The variances of the forces was also estimated by the average values in the eighteen measured loads.

$$\mathscr{D}(\mathbf{c}) \approx a^{-1} \cdot (\mathbf{c}\,\Sigma\,\mathbf{c}^T)^{3/2}(4.84 + 0.025\kappa_e + 3.486\kappa_e^{1/2} - 2.158\kappa_e^{1/3}), \qquad (13)$$

where Σ is the covariance matrix of the loads, i.e. Σ has the variances of the loads on the diagonal and covariances between the loads out of the diagonal.

5 Example

In this section the accuracy of the formula (13) for the expected damage index is investigated. We consider the forces $F_y(t)$, $F_z(t)$. The constants $\mathbf{c} = [\cos(\theta)\ \sin(\theta)]$, $0 \leq \theta < 2\pi$, representing all possible linear combinations, are used.

In the real world observation experiments 18 multiaxial loads were registered at the same field but at different locations. (One of them is presented in Figure 1.) It is assumed that the field is homogeneous and hence an average of observed damage indexes $D^{obs}(\mathbf{c})$ is computed and taken as the damage index for the whole field. In Figure 7 average observed damage index $D^{obs}(\mathbf{c})$ is shown as thick solid line.

One interesting question is whether parameter values of the Laplace model vary in the field. In order to investigate this question the psd parameters a_{Fy}, a_{Fz}, kurtosis κ_{Fy}, κ_{Fz} and covariance matrices Σ were estimated, for each of the 18th measurements. Using the 18 Laplace models the average damage index was estimated using MC method. The resulting index is given in Figure 7 as the dashed line. Finally $\mathscr{D}(\mathbf{c})$

was computed using (13) with average value of parameters a, κ, and matrix Σ. The result is shown in the figure as a thin solid line. The three indexes are very close to each other and we conclude that Laplace model with common values of parameters is representative for the whole field.

6 Conclusions

The multivariate Laplace model proves to be useful for studying damages resulting from multiaxial loads. It summarizes in a very small number of parameters important features of the loads that are affecting damage. This efficiency in parameters allows for description of customer (market) variability by means of probability distributions of the parameters. The model is suitable for modeling loads containing transients.

7 Acknowledgments

The authors are thankful to Väderstad-Verken AB for supplying the cultivator data. The second author acknowledges Riksbankens Jubileumsfond Grant Dnr: P13-1024 and Swedish Research Council Grant Dnr: 2013-5180, while the third author acknowledges Knut and Alice Wallenberg stiftelse for their support.

References

1. P.A. Brodtkorb, P. Johannesson, G. Lindgren, I. Rychlik, J. Rydén, and E. Sjö. Wafo - a matlab toolbox for analysis of random waves and load. *Proc. 10th Int. Offshore and Polar Eng. Conf., Seattle*, 3:343–350, 2000.
2. A. Bengtsson and I. Rychlik. Uncertainty in fatigue life prediction of structures subject to gaussian loads. *Probabilistic Engineering Mechanics*, 24:224–235, 2009.
3. A. Palmgren. Die Lebensdauer von Kugellagern. *VDI Zeitschrift*, 68:339–341, 1924.
4. M.A. Miner. Cumulative damage in fatigue. *J. Appl. Mech.*, 12:A159–A164, 1945.
5. I. Rychlik. A new definition of the rainflow cycle counting method. *Int. J. Fatigue*, 9:119–121, 1987.
6. A. Beste, K. Dressler, H. Kötzle, and W.Krüger. Multiaxial rainflow - a consequent continuation of professor tatsuo endo's work. *The Rainflow Method in Fatigue: The Tatsuo Endo Memorial Volume*, 1992.
7. K. Bogsjö, K. Podgórski, and I. Rychlik. Models for road surface roughness. *Vehicle System Dynamics*, 50:725–747, 2012.
8. S. Kotz, T.J. Kozubowski, and K. Podgórski. *The Laplace distribution and generalizations: A revisit with applications to communications, economics, engineering and finance.* Birkhäuser, Boston, 2001.
9. I. Rychlik. Note on modeling of fatigue damage rates for non-gaussian stresses. *Fatigue Fracture of Engineering Materials Structures*, 36:750–759, 2013.
10. M. Kvarnström, K. Podgórski, and I. Rychlik. Laplace models for multi-axial responses applied to fatigue analysis of cultivator. *Probabilistic Engng. Mechanics*, 34:12–25, 2013.